Soft Matter

Accepted Manuscript

ROYAL SOCIETY OF CHEMISTRY

www.rsc.org/softmatter

Aqueous foams stabilized by chitin nanocrystals

Maria V. Tzoumaki[a,b*], Dimitrios Karefyllakis[b], Thomas Moschakis[c], Costas G. Biliaderis[c], Elke Scholten[b]

a. Department of Food Science and Technology, Perrotis College, American Farm School, Marinou Antipa 54, P.O. Box 23, 551 02, Thessaloniki, Greece

b. Physics and Physical Chemistry of Foods, Wageningen University, P.O. Box 17, 6700AA Wageningen, The Netherlands

c. Department of Food Science and Technology, School of Agriculture, Aristotle University of Thessaloniki, GR-541 24, P.O. Box 235, Thessaloniki, Greece

* corresponding author: maria.tzoumaki@wur.nl,

Abstract

The aim of the present study was to explore the potential use of chitin nanocrystals, as colloidal rod-like particles, to stabilize aqueous foams. Chitin nanocrystals (ChN) were prepared by acid hydrolysis of crude chitin and foams were generated mainly by sonicating the respective dispersions. The foamability of the chitin nanocrystals was evaluated and the resulting foams were assessed for their stability, in terms of foam volume reduction and serum release patterns, during storage. Additionally, the samples were studied with light scattering and optical microscopy in order to explore the bubble size distribution and morphology of the foam. Nanocrystal concentration and charge density was varied to alter the packing of the crystals at the interface. At low concentrations of ChNs, foams were stable against coalescence and disproportionation for a period of three hours, whereas at higher concentrations, the foams were stable for several days. The enhanced stability of foams prepared with ChNs, compared to surfactant-stabilized foams, can be mainly attributed to the irreversible adsorption of the ChNs at the air-water interface, thereby providing Pickering stabilization. Both foam volume and stability of the foam were increased with an increase in ChNs concentration, and at pH values around the chitin's pK_a (pH 7.0). Under these conditions, the ChNs show minimal electrostatic repulsion and therefore a higher packing of the nanocrystals is promoted. Moreover, decreased electrostatic repulsion enhances network formation between the ChNs in the aqueous films, thereby providing additional stability by gel formation. Overall, ChNs were proven to be effective in stabilizing foams, and may be useful in the design of Pickering-stabilized food grade foams.

1. Introduction

Foams are of great practical interest because of their extensive occurrence in the food, pharmaceutical and cosmetic industry. These aerated systems, especially aqueous foams, are usually stabilized by low molecular weight (LMW) surfactants or proteins, but they often suffer from low stability due to many destabilization mechanisms that take place.[1,2] A promising alternative for enhancing foam stability is the utilization of solid particles. In the last years some considerable amount of work has been performed on investigating the potential of particles as foam stabilizers.[3-7] The ability of particles to stabilize interfaces, either oil-water or air-water, has been known already for more than a century, and particle-stabilized interfaces were first reported by Ramsden in 1903.[8] The work was then continued by Pickering in 1908,[9] after whom this stabilization mechanism was named.

The most striking feature of colloidal particles is their ability to adsorb irreversibly at interfaces,[10] rendering them extremely effective as foam stabilizers. The free energy of spontaneous desorption is predicted to be of the order of several thousand kT.[11-13] The energy of adsorption, apart from the size, is significantly determined by the wetting properties of the solid particles, expressed as a contact angle, θ, at the interface. For an angle of 90° the highest degree of stabilization is obtained. The angle depends mainly on the hydrophobicity of the particles. For proper adsorption, the particles should not be too hydrophilic, contact angles < 90°, and not too hydrophobic, contact angles > 90°. For proper wetting ability, this denotes that once the particles are at the interface, they are effectively and irreversibly adsorbed, in marked contrast to surfactant molecules that adsorb and desorb reversibly. As the particles are adsorbed at the interface, they have the ability to form a close-packed structure at the gas–liquid interface, creating a 'colloidal barrier'. This densely packed interfacial layer can retard or even completely inhibit the destabilization of foams caused by bubble coalescence and coarsening (disproportionation).[3,13-17] It has been shown that the particle-stabilized bubbles can resist disproportionation for days or weeks,[14,15] compared to a life time of less than an hour for the respective surfactant or protein-stabilized bubbles.[14] Another distinct difference compared to surfactants, is that the adsorption of solid particles to fluid/liquid interfaces does not always cause a drop in the interfacial tension.[18]

The particles that have been mostly used for Pickering stabilization are commonly of inorganic nature, like silica,[10,19,20] clays[21] and latexes.[22] Beside different materials, also particles with different geometry have been studied in literature,[23] and so far the majority of the studies deal with spherical particles, while few examples of anisotropic particles have been reported. Additionally, there are very few cases of particles that are already food-grade, like fat crystals,[24,25] as the majority of the particles used so far cannot be used in the food industry. An attractive alternative source to these non-food grade materials are natural biopolymers, such as polysaccharides. Some examples of such polysaccharide-based particles as Pickering stabilizers have been reported in literature, like cellulose fibres[26-28] and modified starch granules.[29] Recently, also other biomaterials, such as shell-fish waste and insects, have been used to derive colloidal particles, namely chitin nanocrystals. These nanocrystals have been shown to exhibit large capacity in stabilizing oil-in water emulsions even with relatively large oil droplet sizes.[30] Moreover, these emulsions were shown to be particularly stable under digestive conditions and able to slow down the lipid digestion process, indicating the presence of very stable and dense interfaces.[31] The large stability was attributed to the Pickering mechanism. The chitin nanocrystals can be produced from hydrolysis of raw chitin in acidic aqueous solutions, and the resulting dispersions consist of rod-like particles with average dimensions around 240 nm in length and 18 nm in diameter, as determined in the work of Tzoumaki et al..[32] The chitin particles may possess positive charges at their surface due to the protonation of aminogroups present.[32] Although their ability to stabilize oil-water interfaces has been reported, no information is yet available about the ability of these nanoparticles to stabilize air-water surfaces.

Therefore, the aim of the present work was to investigate the potential of chitin nanocrystals (ChNs) as foam stabilizers. We investigated the factors that may influence the properties of the respective foams, such as ChN concentration and charge density to reveal possible mechanisms behind their ability to stabilize air-water interfaces. Charge density was varied by changing pH. Foams were produced by applying sonication to aqueous ChN dispersions, and the produced foams were studied for their stability by means of visual observations, optical microscopy and light scattering, in an attempt to understand the underlying stabilization mechanism(s).

2. Materials Methods

2.1. Materials

Crude chitin from shrimp shells, as well as all other chemicals, such as potassium hydroxide, sodium acetate, glacial acetic acid, sodium chlorite, sodium chloride, hydrochloric acid (concentrated 37% v/v), sodium azide, absolute ethanol were purchased from Sigma Chemicals (St Louis, USA). A dialysis bag (Spectra/Por® 4 with MWCO 12-14kD) was obtained from Spectrum laboratories (California, USA).

2.2. Chitin nanocrystal (ChN) preparation

Aqueous stock dispersions of chitin nanocrystals (ChN) were prepared by acid hydrolysis (3 N HCl, 95°C, 90 min) of the original raw material of crude chitin from shrimp shells. Detailed information on bleaching (with sodium chlorite) and acid hydrolysis are given elsewhere.[32] The solid content of the stock dispersion was determined gravimetrically by drying the samples at 50°C until a constant weight was obtained; the total solids content of the stock dispersion was approximately 6%. The final pH of the stock dispersion was adjusted to 3.0 with 1 N HCl and the dispersion was sonicated for 4 minutes before any use, in order to assure that the ChN nanocrystals are not aggregated.

Samples with ChN concentrations ranging from 0.005 to 5% were prepared by adding acidified distilled water with pH 3.0. The pH of the samples was further adjusted by either adding 0.1 N HCl and/or 0.1 N NaOH.

2.3. Foam generation

Preliminary experiments showed that foams cannot effectively be produced by low energy input techniques, such as air injection. Therefore, a more efficient method was selected, and for most of the experiments this was found to be ultrasonication. ChN dispersions were subjected to ultrasonication treatments using a long sonication horn (1/8″ Tapered Microtip© 101-148-062, Branson, USA). The duty cycle was adjusted at 90%, the frequency at 60 kHz and treatment duration was 20 s. All the experiments were performed at room temperature (~25˚C). To increase the initial adsorption of the nanocrystals onto the interfaces, a small amount of ethanol (1%) was added. We assume that the ethanol

evaporates relatively fast after frothing, without affecting the final properties of the produced foams.

2.4. Particle charge

The zeta potential of ChN dispersions was determined with dynamic light scattering (Zetasizer ZS, Malvern, UK) and the utilization of a disposable capillary cell (DTS1070) at 20˚C. The ChN concentration of the samples was adjusted to 0.1 % (w/w) by diluting the samples with an aqueous solution of the respective pH and the experiments were performed in triplicates.

2.5. Maximum foamability

After the foams from different dispersions were produced under the same conditions, their height (in cm) was recorded. The dispersion volume for all the measurements was kept constant (60mL). All the experiments were performed at constant temperature (~25˚C) and in triplicates. The foamability was then expressed as the foam volume, FA, in percentage of the initial dispersion volume as:

$$FA_{volumetric} = \frac{FoamVolume}{DispersionVolume} \times 100\,(\%) \quad (1)$$

2.6. Foam stability

The resistance of the produced foams towards destabilisation was monitored visually (using graduated tubes), with light scattering (Foam scan, Teclis Instruments, France) and microscopy. For visual observations, a fixed sample volume (60 mL) was transferred into the graduated tubes and the sample was sonicated (10s) until a foam height of 25cm was reached. The height of the foam was visually recorded every few minutes, over a three hour period. Foam stability, FS, is expressed as:

$$FS_{volumetric} = \frac{Foam\,Volume}{Initial\,FoamVolume} \quad (2)$$

Moreover, the level of the serum was recorded in time and the results were expressed as the serum volume height (meniscus height) over time.

Regarding the foam scan measurements, samples were initially prepared by sonication and subsequently poured into the foam scan column where a video camera recorded the structure of the foam through time. Using an image analysis software (Cell Size Analysis, CSA, Teclis Instruments) the number and the size of the bubbles were calculated, and the changes in bubble size distribution were determined both at the time of preparation and after 1 hr.

2.7. Optical microscopy

The respective aqueous foams prepared by handshaking were observed using an optical microscope with a polarized lens (Axioskop, Carl Zeiss AG, Oberkochen, Germany), equipped with a camera (Axiocam HRc, Carl Zeiss AG, Oberkochen, Germany).

2.8. Scanning Electron Microscope observations

Scanning Electron Microscopy (SEM) (FEI Maggalan 400, Hilsboro, OR, USA) was conducted on dried samples sputter-coated with platinum or iridium, operated at 2 kV.

3. Results and discussion

3.1. *Effect of ChN concentration*

The first attempts to produce foams from ChN aqueous dispersions were based on incorporating air through simple air injection. For dispersions with low ChN concentrations (<1% w/w), foam fabrication was not possible. When dispersions of higher ChN concentrations were used (>2%), foams could be produced, but with relatively large bubble size. It is worth mentioning that even though the bubble size was large, these samples were stable over a period of a few days. This finding indicates that the chitin nanocrystals stay at the interface for long periods once adsorbed, but the adsorption process may not be sufficient. The low foamability of particles is not uncommon, and in general, particle-

stabilized foams are more difficult to be prepared compared to foams stabilized by common surfactants by simply blowing air into the dispersion. Colloidal particles are much larger than common surfactants and therefore their diffusion rate is lower. Particles therefore have less probability to adsorb to the interface while the foam and the accompanying interface is created. Additionally, as the particles are also heavier than common surfactants, they are more prone to be influenced by gravity and drainage phenomena.

To increase the foamability of particle dispersions, other techniques involving larger energy inputs are required, like energetic shaking and turbulent mixing.[33] Here, we have used sonication as a high energy input technique in order to produce a better dispersion of ChNs which might lead to a higher surface coverage (packing). In Fig. 1, a characteristic foam produced from a 3% ChN aqueous dispersions by air injection (Fig. 1a) and sonication (Fig. 1b) is shown. It can clearly be seen that the bubble size of the foams prepared with air injection is in the range 0.2-0.5 cm, while the bubbles created by sonication appear to be considerably smaller.

Therefore, to increase the foamability of the dispersions, sonication was used as a more effective foaming method in the rest of the experimentations. In order to explore the effect of ChN concentration on the foam properties, a wide range of ChN concentrations was used for producing foams. The pH of the dispersions was set at 7.0, which is close to the iso-electric point of chitin. At this pH, the nanocrystals have limited charge density, and therefore no large electrostatic repulsion between the particles is expected. The lower limit was set at 0.1% (w/w) of ChN, as the foams collapsed almost immediately for lower concentrations. The higher limit was set at 1%, as for higher concentrations, the continuous phase viscosity was increased to such extent that foam formation was partially restricted. Consequently, a set of ChN foams with a range of concentrations from 0.1 to 1.0% was produced. After preparation, air bubbles rapidly started to accumulate at the top of the tube (i.e., creaming) due to the high density difference between the phases. As can be seen in Fig. 2, foamability was related to ChN concentration. As the ChN concentration increased, an increase in the aqueous foam volume was observed. A higher ChN concentration possibly enabled the local adsorption of a greater amount of particles at the air–water interface, leading to the fabrication of a larger air-water interface. An increase in foamability as a function of colloidal particle concentration has been reported in many works; e.g. for partially hydrophobic silica spheres,[3,15] crystalline sodium chloride particles,[34] laponite disk-

like particles,[35] zirconium phosphate nano-sheets,[5] microparticles from hydrophobic cellulose,[27] and solid particles from surfactants.[36]

The foamability in terms of their initial bubble size was also examined. Fig. 3 shows images of foams with different ChN concentrations ranging from 0.1 to 0.7% (w/w), obtained by foamscan, and the corresponding size distribution of the air bubbles. With increasing ChN concentration (Fig. 3a to d), it is obvious that the number of larger air bubbles, as represented by the right peak in the bimodal size distribution profile, decreases and at the same time, the left peak becomes more and more distinct, indicating a shift towards smaller bubble sizes. In general, a smaller bubble size is related to a larger total air-water surface and therefore indicates that more particles are available for adsorption. Indeed, the results show that the ChN concentration strongly influenced the resulting bubble size. For a concentration of 0.7%, surface coverage was already sufficient to provide relatively small bubbles.

Furthermore, in order to analyze the stability of the ChN-stabilized foams, the foam volume, expressed as the fraction FS, (Fig. 4a) and the serum volume (Fig. 4b) were followed in time. In general, there is a clear dependence of the changes in foam volume and serum volume with time on ChN concentration. As it is depicted in Fig. 4a and 4b, the higher the ChN concentration the slower the foam collapse, and therefore a higher foam stability and a corresponding slower serum release. For ChN concentrations of 1.0 %, it can be seen that the foam volume remained almost constant for more than 180 min, and even for several days (data not shown). This is much longer than foams prepared with proteins or low molecular weight surfactants, which are generally stable for minutes only.[2] At this high concentration of ChN, the solution was very opaque, hindering the observation of the serum release levels. However, in general we see that for higher concentrations, less changes in serum volumes are observed. This indicates that more liquid remains present in the aqueous films between the air bubbles, and drainage is slowed down. These results show that there is a relation between the initial bubble size and the foam stability. For a higher interfacial coverage, smaller bubbles are obtained, serum release is mostly prevented, and higher foam stability is obtained.

The increased stability of the ChN-stabilized foams can be attributed to the ability of ChN particles to irreversibly adsorb at the air-water interface that renders them stable against destabilizing mechanisms, such as coalescence and disproportionation. As previously

mentioned, the adsorption energy required to remove the particles from the interface is of the order of several thousands of k_BT, making them very difficult to desorb from the interface.[5,37,38] A decrease in interfacial area by merging of bubbles is therefore restricted, as decrease in area would require desorption from the interface. Even if the interface is not completely covered, the pressure in the air bubbles (exerted by the curvature to provide a capillary pressure) would not be sufficient to break the interfacial film. As the ChN concentration increases, adsorption of a larger amount of particles leads to an increased interfacial coverage and closer packing of the particles. The close packing leads in this way to the formation of a colloidal armor, thus leading to more foam stabilization. As the interface becomes more packed and the distance between the particles decreases, the interface becomes more resistant to folding, and gas diffusion is decreased, thereby inhibiting both coalesce and disproportionation. For all concentrations of ChN used, the experiments show that the bubble size and the bubble size distribution did not change within the time span of the experiments (1 hr), indicating that they were fairly stable against disproportionation and coalescence (data not shown). Thus, even though maximum packing of particles at the surface may not have been obtained yet, partial packing provided already the required interfacial properties to prevent the destabilization mechanisms.

Stability against mechanisms as bubble coalescence and disproportionation as well as prolonged lifetimes have also been observed in many cases of hydrophobic silica-stabilized foams.[14,15,17] To study the changes in the interfacial area, techniques such as X-ray tomography and multiple light scattering have been used to follow the ageing of different foams. In the case of hydrophobically modified silica nanoparticles, these techniques showed that bubble size evolves little with time provided the concentration of the silica particles in the aqueous bulk phase is high enough.[38] This indicates that indeed the interfacial area does not change anymore once the particles are adsorbed. It is worth mentioning that ChNs possess a characteristic that the commonly used spherical particles do not have, and that is their rod-like anisotropic shape.[32] Up to now, it has been shown that the shape of the particle plays a dominant role in the stability of interfaces, since the attractive interactions among anisotropic particles are higher compared to spherical ones, leading in this way to higher interfacial packing and higher mechanical rigidity.[39-43] Even for particles with similar wettability and size, ellipsoidal particles were shown to produce more

stable interfaces than spherical particles.[40] There are examples of anisotropic particles that have been used such as nano-sheets,[5,6] microrods,[41,44] and ellipsoids.[40]

Besides the interfacial stabilization, another important factor that may play a role in the enhanced stability of the ChN foams, is the network formation by ChNs within the liquid lamellae. Due to the low adsorption kinetics,[31] the particles will partly remain present in the aqueous bulk phase. During the foam formation, these particles are transferred into the liquid films separating the air bubbles. Upon partial drainage of the liquid from the films, the concentration of the ChNs may increase. As is already known, ChN aqueous dispersions transform from an isotropic-liquid towards a nematic gel-like behaviour with increasing solid particle concentration. Such a isotropic-nematic phase transition has been shown to occur at ChN concentrations of approximately 1.8% (for pH values close to 7), slightly higher than the concentrations used in our foams.[32] In the case of ChN-stabilized emulsions, such a gel-like behavior was already observed at concentrations of 0.3%, indicating that such nematic structures may already be formed at lower concentrations when the particle orientation can be influenced by the presence of an interface.[30] The ChN particles have the tendency to align parallel due to entropic reasons, and it has been found that in such a parallel configuration attractive interactions, mainly van der Waals, are further enhanced.[32] The presence of a network within the liquid lamellae may limit liquid drainage from the film, thereby retaining high film thickness, leading to a higher stability of the aqueous foams. To test the presence of such nematic structures within the liquid films, we have investigated the optical properties of a foam, created from hand-shaking a 1% ChN dispersion. In Fig. 5, a characteristic image of the foam from crossed polarized microscopy, is shown. Intense birefringent regions are observed at the bubbles' surface, indicating that the ChN are present in an orderly fashion at the air-water interface. Additionally, some strong birefringent regions are observed in the continuous phase, similar to the ones observed for gel-like ChN dispersions.[32] The ChN particles appear to form nematic structures within the liquid lamellae, and may aid in the stability of the foams. The formation of nematic structures leads to enhanced viscosity of the liquid phase, and may lead to more gel-like properties when the structures are able to form a connecting network. At this point, it is worth pointing out that such network formation is a typical characteristic of particles in general, but is more pronounced in the case of anisotropic particles, compared to spherical particles.[14,41] For anisotropic particles, like sheets or polymer microrods[41] network formation

can occur, as they can entangle, overlap, or form orientated domains at relatively low concentrations, as is shown for the rod-like ChNs in the present study. This network formation provides an extra barrier against drainage and collapse of the foam. During drainage of the liquid film and consequent increase of the ChN concentration, such a network could be formed, and may even lead to formation of solid-like lamellae.

Apart from the optical microscopy, scanning electron microscopy studies were performed, in order to clarify further the stabilization mechanism of the ChN foams. Fig. 6a gives a representation of a foam prepared at pH 7.0, and in Fig. 6b the respective magnification near the interface is shown. The image reveals that the ChNs have a parallel nematic orientation at the interface and is extended in the continuous phase, which was also concluded from the polarized optical micrographs. However, no direct conclusions can be drawn, as these interfaces were partly manipulated by a drying step used to prepare the samples. The drying step may induce strong aggregation of the ChN particles at the interface and the bulk phase and could induce artefacts in the micrograph obtained with SEM. Therefore, it may not represent the situation of the liquid foams. Moreover, due to the high degree of aggregation, it is difficult to distinguish the particle situated at the interface from the particles in the continuous bulk phase, and to extract information on their packing orientation.

In Fig. 7, a representative image of a fresh foam (left) is given, and images of foams after 1 day of preparation for different ChN concentrations (right). For freshly prepared foams, the visual appearance of the foam is independent on the ChN concentration (in the range of 0.1-1.0%). However, after 1 day the samples with relatively low (0.2%) ChN concentration, presented a typical foam evolution pattern, for which larger bubbles cream towards the top, and the liquid drains down. In this case, the concentration of ChN was probably not high enough to gain a more viscous or gel-like behavior in the liquid phase and thereby reduce drainage and other destabilization mechanisms. In the case of higher ChN concentration (1.0%), a different behavior was observed. The total volume of the foam remained practically unchanged, even after a few days, but the foam became sticky and solid-like over time. This is likely to be due to the increased viscosity of the liquid films and subsequent network formation of the ChN in the liquid film. Besides wall-foam stickiness, foam solidification was observed as drainage was slowly completed, and the resulting film gelled (and solidified). The formation of such a solid foam has been reported in similar

systems, where foams where stabilized solely with polymer latex particles.[45] The formation of a more solid foam confirms that indeed network formation of ChN nanocrystals takes place within the liquid lamellae, thereby providing additional stability to the foam.

3.2. Effect *of pH*

As the packing of the ChNs seems to play an important role, repulsive (electrostatic) interactions between the nanocrystals may influence the foam stability. Electrostatic interactions can be tuned by altering the pH, as this changes the charge density of chitin. Increased electrostatic repulsions would probably lead to less packing of the ChNs at the interface and less network formation within the lamellae, rendering the respective foams less stable. The zeta-potential of the samples at pH values between 3.0 and 8.0 was initially measured, in order to investigate the effect of pH of the aqueous medium on the ChNs' charge density (Fig. 8). At acidic pH values the particles bear strong positive charges; i.e. 50 mV at pH 3.0. These results were expected since it is known that chitin possesses amino groups in its structure, and in acidic media these are protonated to form $-NH_3^+$. The charge of the dispersion was neutralised as the pH increased to values of 7.0 as a result of approaching the chitin's pK_a value of 7, as reported in literature.[46] Surprisingly, the net charge presented negative values as the pH increased to 8.0, i.e., the zeta potential was found to be -20 mV. Although these negative values have not been reported extensively in literature, there are a few cases for which negatively charged chitin at pH levels above the pK_a were reported.[47,48] Liu and co-workers reported values around -30 mV at pH 10.0, and they attributed the heteropolyelectrolyte property to both the amino groups (positively charged at acidic pH), and carboxylate groups (negatively charged at alkali pH) generated from the oxidation of alcoholic groups during bleaching.[48]

Foams at different pH values were produced at a constant ChN concentration of 0.7% w/w, and the total foam volume (foamability FA) and foam volume decay over time (foam stability FS) were recorded. For samples with pH values of 3 and 4, foam formation was not possible. At these pH values, the charge density is high, and therefore the strong electrostatic repulsion between the particles prevents sufficient particle packing. Fig. 9 shows the results for conditions that did lead to foam formation. It is shown that the samples with pH values of 5 and 6 exhibited low foamability, while the maximum foamability

was observed for the samples with pH of 7 and 8. In the case of the foam stability, presented in Fig. 10, we see a similar trend. The foams were more stable as the pH value increased from 5 up to 7, related to a decrease in the positive charge density. At higher pH values, both the foam fraction (Fig. 10a) and the serum release (Fig. 10b) showed smaller changes**.** For samples with pH 8, when the samples became slightly negative, the foam stability was slightly lower compared to the foam formed at pH 7.

At pH values around 7, the ChNs present minimal charge and this may influence the foam formation and stability due to different reasons. At low or minimal charge, the particles might present a more hydrophobic character. A higher hydrophobicity would decrease the solubility in the aqueous bulk phase, at the same time increase the adsorption onto the air-water surface, thus rendering in this way the less charged ChNs more capable to form foams. This effect of changes in solvent affinity has also been discussed for ethylcellulose particle foams.[37] Jin and co-workers proposed that changes in pH or ionic strength can lead to changes in the particle contact angle, thus making the particles more hydrophobic. Another reason would be the packing ability of the particles. At pH 7, the particles have reduced electrostatic repulsion, and are therefore able to pack closer at the interface. As discussed before, closer packing leads to ordering of the nanocrystals and the ChN dispersions are known to exhibit a stronger gel-like behaviour.[32] The closer packing will lead to more surface coverage at the interface, and thereby providing a more efficient colloidal barrier against air diffusion and coalescence. As already discussed, enhanced network formation in the liquid lamellae also plays an important role in the stability of the ChN foams. For the samples with increased charge density of the chitin nanocrystals, lower foamability and stability was noted, even though the same concentration of nanocrystals was used. The increased electrostatic repulsion between the ChNs reduce their ability to adsorb closely at the interface. Additionally, no network formation is present in the lamellae, and therefore they retain their liquid behavior. The absence of gel formation in the lamellae and a less efficient interfacial barrier results in foams with much lower stability. Moreover, once a few ChNs particles are absorbed at the interface, they may repel the new particles approaching the surface. This indicates that for particle-stabilized foams, the packing ability and the concomitant high viscosity in the liquid film is the dominant factor determining their stability (shelf-life).

4. Conclusions

The aim of this study was to investigate the potential of chitin nanocrystals (ChNs) as foams stabilizers. In general, the results show that ChNs, even without the presence of surfactants, are quite effective in stabilizing aqueous foams against coalescence and disproportionation, over a period of three hours, and at higher ChNs concentrations even for days. The enhanced stability of foams prepared with ChNs, compared to surfactant-stabilized foams, can mainly be attributed to a Pickering mechanism, according to which the ChNs are irreversibly adsorbed at the air-water interface. Both foamability and foam stability were mainly governed by the ability of the nanocrystals to pack closely at the interface to provide a colloidal barrier, as well as to provide gel-like properties in the liquid lamellae. The highest foamability and stability of the foams was observed at increased ChNs concentrations, and at pH values around the chitin's pK_a (pH 7.0). Under these conditions, the ChNs exhibit minimal electrostatic repulsion, and therefore packing of the nanocrystals is promoted. The results of the present study might provide opportunities for the design of novel food grade aqueous foams, with enhanced stability, that could be used in the food, the pharmaceutical or cosmetics industry.

References

1. T. N. Hunter, R. J. Pugh, G. V. Franks and G. J. Jameson, *Advances in Colloid and Interface Science*, 2008, **137**, 57-81.
2. R. J. Pugh, *Advances in Colloid and Interface Science*, 1996, **64**, 67-142.
3. T. Kostakis, R. Ettelaie and B. S. Murray, *Langmuir*, 2006, **22**, 1273-1280.
4. E. Dickinson, *Current Opinion in Colloid & Interface Science*, 2010, **15**, 40-49.
5. J. S. Guevara, A. F. Mejia, M. Shuai, Y. W. Chang, M. S. Mannan and Z. D. Cheng, *Soft Matter*, 2013, **9**, 1327-1336.
6. Z. D. Cheng, A. F. Mejia, J. S. Guevara, Y. W. Chang and M. Shuai, *Abstracts of Papers of the American Chemical Society*, 2013, **245**.
7. N. Schelero, A. Stocco, H. Mohwald and T. Zemb, *Soft Matter*, 2011, **7**, 10694-10700.
8. W. Ramsden, *Proceeding of the Royal Society of London* 1903, **72**, 156.
9. S. U. Pickering, *Journal of Chemical Society*, 1908, **91**, 2001-2021.
10. B. P. Binks and T. S. Horozov, *Angewandte Chemie-International Edition*, 2005, **44**, 3722-3725.
11. E. Dickinson, *Trends in Food Science & Technology*, 2012, **24**, 4-12.

12. R. Aveyard, B. P. Binks and J. H. Clint, *Advances in Colloid and Interface Science*, 2003, **100**, 503-546.
13. R. Ettelaie and B. Murray, *Journal of Chemical Physics*, 2014, **140**.
14. Z. P. Du, M. P. Bilbao-Montoya, B. P. Binks, E. Dickinson, R. Ettelaie and B. S. Murray, *Langmuir*, 2003, **19**, 3106-3108.
15. E. Dickinson, R. Ettelaie, T. Kostakis and B. S. Murray, *Langmuir*, 2004, **20**, 8517-8525.
16. T. S. Horozov and B. P. Binks, *Colloids and Surfaces a-Physicochemical and Engineering Aspects*, 2005, **267**, 64-73.
17. A. C. Martinez, E. Rio, G. Delon, A. Saint-Jalmes, D. Langevin and B. P. Binks, *Soft Matter*, 2008, **4**, 1531-1535.
18. E. Vignati, R. Piazza and T. P. Lockhart, *Langmuir*, 2003, **19**, 6650-6656.
19. J. Frelichowska, M. A. Bolzinger and Y. Chevalier, *Journal of Colloid and Interface Science*, 2010, **351**, 348-356.
20. B. Braisch, K. Kohler, H. P. Schuchmann and B. Wolf, *Chemical Engineering & Technology*, 2009, **32**, 1107-1112.
21. N. P. Ashby and B. P. Binks, *Physical Chemistry Chemical Physics*, 2000, **2**, 5640-5646.
22. A. J. Morse, S. P. Armes, K. L. Thompson, D. Dupin, L. A. Fielding, P. Mills and R. Swart, *Langmuir*, 2013, **29**, 5466-5475.
23. S. Coertjens, P. Moldenaers, J. Vermant and L. Isa, *Langmuir*, 2014, **30**, 4289-4300.
24. M. Nadin, D. Rousseau and S. Ghosh, *Lwt-Food Science and Technology*, 2014, **56**, 248-255.
25. R. Gupta and D. Rousseau, *Food & Function*, 2012, **3**, 302-311.
26. I. Capron and B. Cathala, *Biomacromolecules*, 2013, **14**, 291-296.
27. H. A. Wege, S. Kim, V. N. Paunov, Q. X. Zhong and O. D. Velev, *Langmuir*, 2008, **24**, 9245-9253.
28. I. Kalashnikova, H. Bizot, B. Cathala and I. Capron, *Langmuir*, 2011, **27**, 7471-7479.
29. A. Yusoff and B. S. Murray, *Food Hydrocolloids*, 2011, **25**, 42-55.
30. M. V. Tzoumaki, T. Moschakis, V. Kiosseoglou and C. G. Biliaderis, *Food Hydrocolloids*, 2011, **25**, 1521-1529.
31. M. V. Tzoumaki, T. Moschakis, E. Scholten and C. G. Biliaderis, *Food & Function*, 2013, **4**, 121-129.
32. M. V. Tzoumaki, T. Moschakis and C. G. Biliaderis, *Biomacromolecules*, 2010, **11**, 175-181.
33. A. Stocco, E. Rio, B. P. Binks and D. Langevin, *Soft Matter*, 2011, **7**, 1260-1267.
34. K. Vijayaraghavan, A. Nikolov and D. Wasan, *Advances in Colloid and Interface Science*, 2006, **123**, 49-61.
35. Q. Liu, S. Zhang, D. J. Sun and J. Xu, *Colloids and Surfaces a-Physicochemical and Engineering Aspects*, 2009, **338**, 40-46.
36. L. K. Shrestha, D. P. Acharya, S. C. Sharma, K. Aramaki, H. Asaoka, K. Ihara, T. Tsunehiro and H. Kunieda, *Journal of Colloid and Interface Science*, 2006, **301**, 274-281.
37. H. J. Jin, W. Z. Zhou, J. Cao, S. D. Stoyanov, T. B. J. Blijdenstein, P. W. N. de Groot, L. N. Arnaudov and E. G. Pelan, *Soft Matter*, 2012, **8**, 2194-2205.
38. A. Stocco, F. Garcia-Moreno, I. Manke, J. Banhart and D. Langevin, *Soft Matter*, 2011, **7**, 631-637.
39. V. R. Dugyala, S. V. Daware and M. G. Basavaraj, *Soft Matter*, 2013, **9**, 6711-6725.

40. B. Madivala, S. Vandebril, J. Fransaer and J. Vermant, *Soft Matter*, 2009, **5**, 1717-1727.
41. R. G. Alargova, D. S. Warhadpande, V. N. Paunov and O. D. Velev, *Langmuir*, 2004, **20**, 10371-10374.
42. J. W. J. de Folter, E. M. Hutter, S. I. R. Castillo, K. E. Klop, A. P. Philipse and W. K. Kegel, *Langmuir*, 2014, **30**, 955-964.
43. P. H. Yang, W. Sun, S. Hu and Z. R. Chen, *Progress in Chemistry*, 2014, **26**, 1107-1119.
44. R. G. Alargova, V. N. Paunov and O. D. Velev, *Langmuir*, 2006, **22**, 765-774.
45. S. Fujii, P. D. Iddon, A. J. Ryan and S. P. Armes, *Langmuir*, 2006, **22**, 7512-7520.
46. J. Li, J. F. Revol, E. Naranjo and R. H. Marchessault, *International Journal of Biological Macromolecules*, 1996, **18**, 177-187.
47. L. Klapiszewski, M. Wysokowski, I. Majchrzak, T. Szatkowski, M. Nowacka, K. Siwinska-Stefanska, K. Szwarc-Rzepka, P. Bartczak, H. Ehrlich and T. Jesionowski, *Journal of Nanomaterials*, 2013.
48. P. Liu, H. Sehaqui, P. Tingaut, A. Wichser, K. Oksman and A. P. Mathew, *Cellulose*, 2014, **21**, 449-461.

Figures

Fig. 1: Foam produced by a) air injection and b) by sonication, of a 3.0% (w/w) ChN aqueous dispersion (pH 7.0)

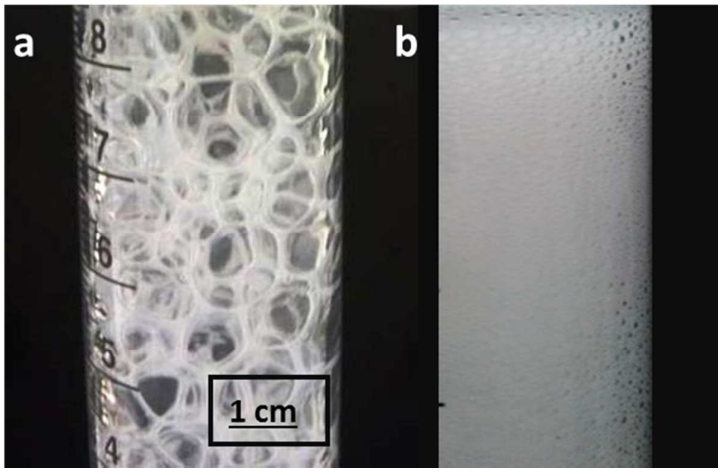

Fig. 2: Foamability of ChN aqueous dispersions with different concentrations at pH 7.0.

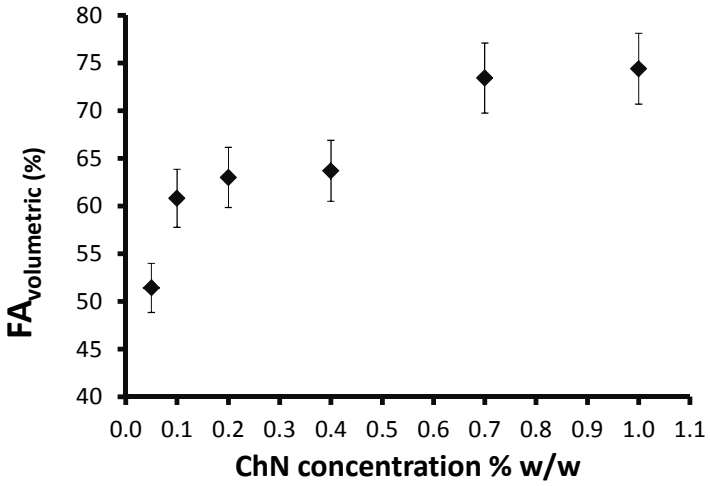

Fig. 3: Bubble size distribution of freshly prepared foam from ChN aqueous dispersions at pH 7.0, with different concentrations a) 0.1 , b) 0.2 , c) 0.4 and d) 0.7% w/w. On the background, the corresponding snapshots from the foam scan are shown.

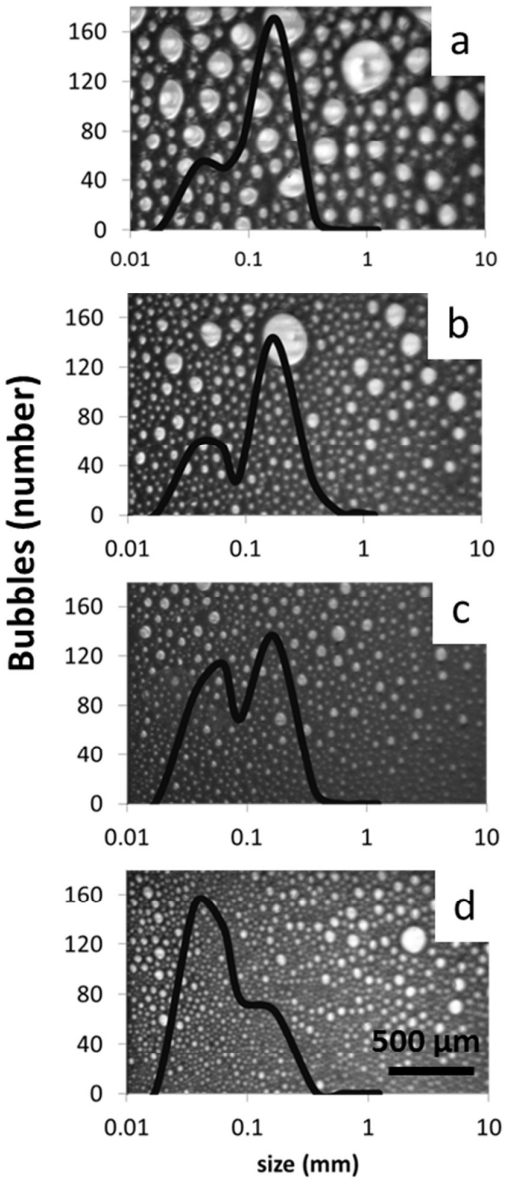

Fig. 4: a) Foam fraction degradation and b) reflux velocity presented as the serum volume as a function of time for samples with increasing ChN concentration (at constant pH 7.0). For a concentration of 1% ChN, no serum volume is given, as a clear interface was not visible.

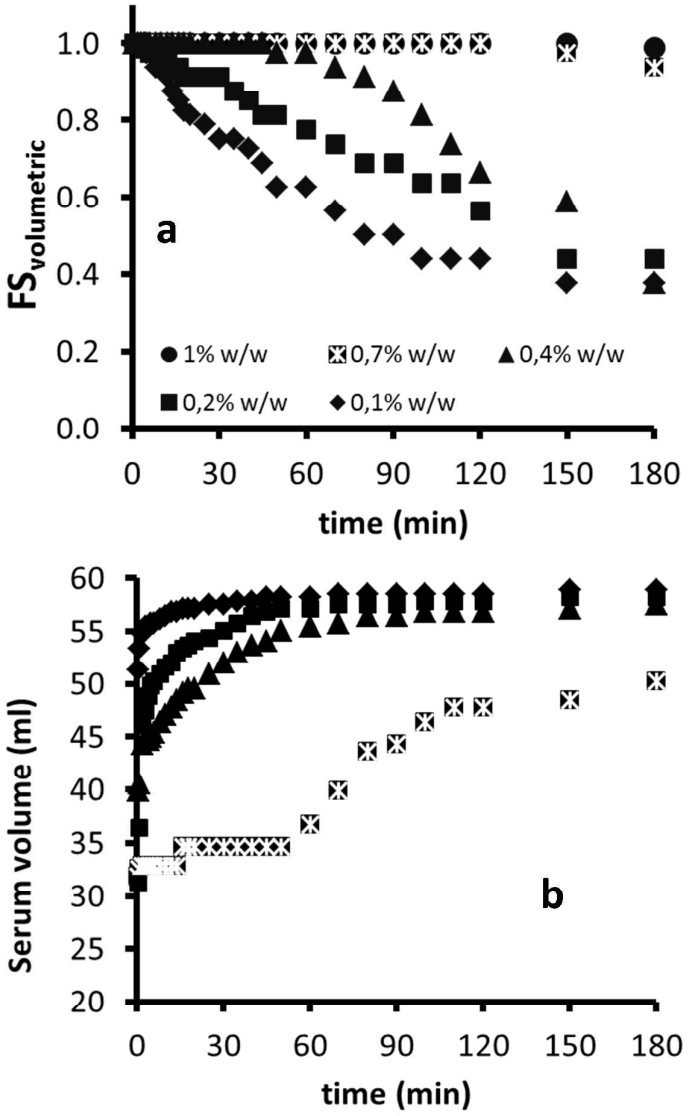

Fig. 5. Typical crossed-polarized optical micrograph of a hand-shaken ChN foam (1% w/w ChN, pH 7.0) Scale bar 100 µm.

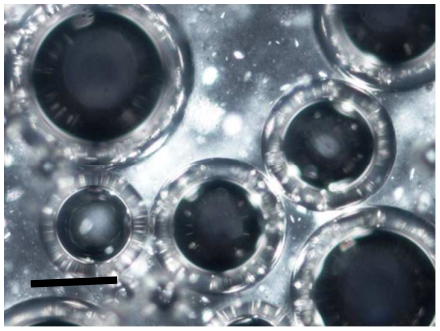

Fig. 6. SEM images of foams stabilized with ChNs after drying, (pH 7.0) (b is the magnified section of a)

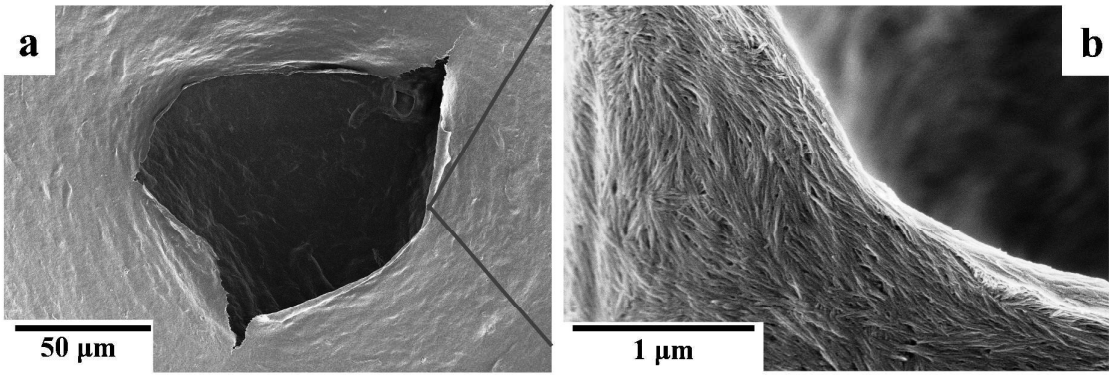

Fig. 7: ChN foams 1 day after preparation (pH 7.0).

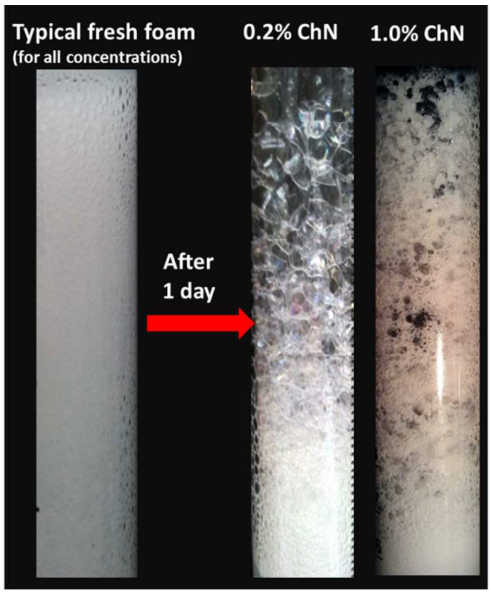

Fig. 8: ChNs zeta potential at different pH values.

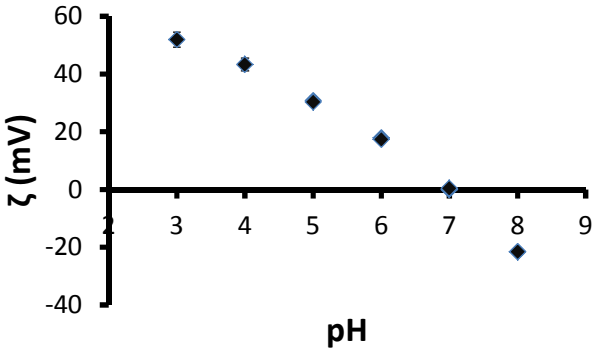

Fig. 9. Influence of pH on maximum foamability of ChN dispersions at constant concentration 0.7% w/w.

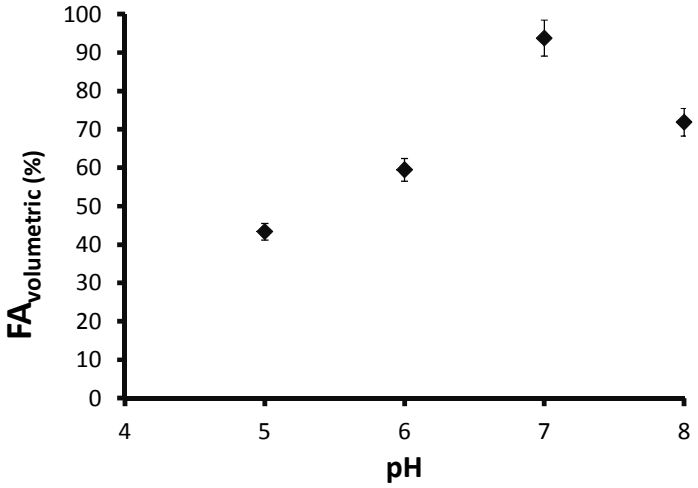

Fig. 10: a) Foam fraction degradation and b) reflux velocity presented as the serum volume as a function of time for samples with a ChN concentration of 0.7% w/w at different pH values.

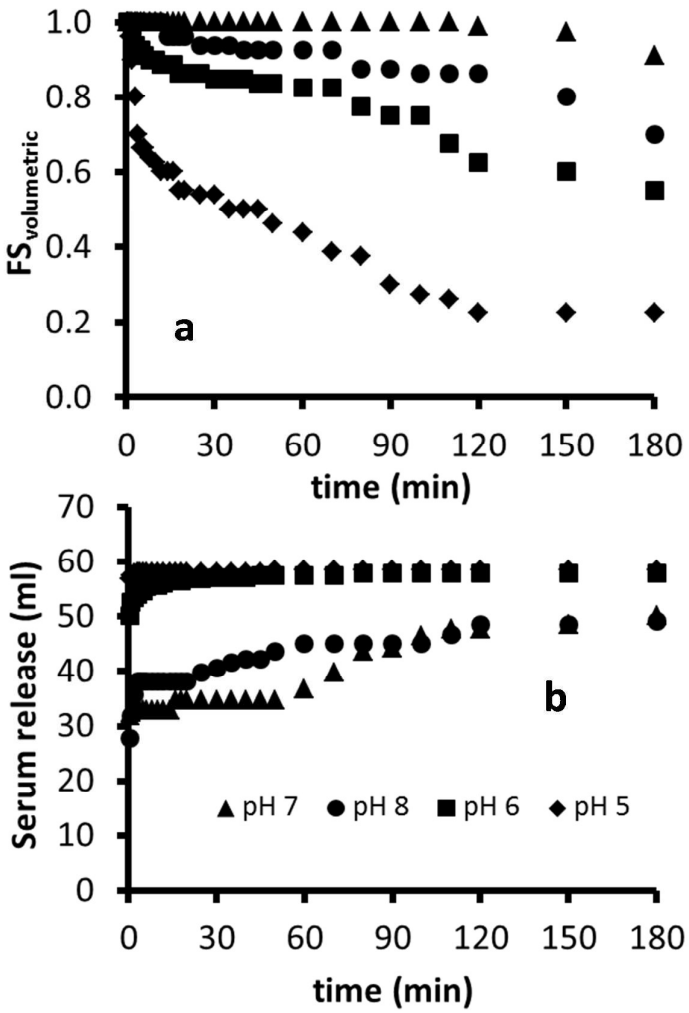

Table of contents

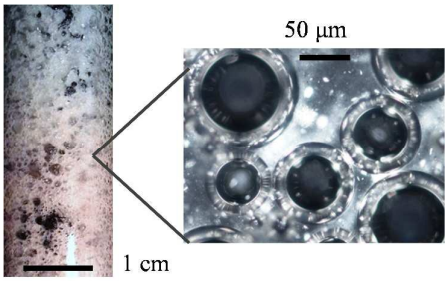

Use of rod-like chitin nanocrystals for providing Pickering stabilization to aqueous foams.